

Summary

We measured electrical impedance spectra of 40 seafloor samples, 30 of which are sulfide-bearing, and 10 are unmineralized host-rock. The resistivity magnitude shows a clear difference between mineralized and unmineralized samples, and also a weak grouping between the different types of mineralization. The imaginary conductivity at 1 Hz indicates an even more pronounced discrimination, suggesting that complex measurements might be useful for exploration purposes. Surprisingly, even under dry conditions the sulfide-bearing samples exhibit significant phase shifts, indicating that an electrolyte is not necessary to generate an IP effect.

Introduction

The electrical properties of continental ore-bearing rocks have been studied extensively (e.g. Pelton et al., 1978). Except for some local studies (e.g. Bartetzko et al., 2006), little is known about seafloor deposits. There is an increasing interest, in particular in seafloor massive sulfides (SMS), which are considered a new source of base metals with economic relevance (e.g. Hannington et al., 2011). Here, we discuss electrical spectra of seafloor samples and investigate potential relationships between SIP parameters and mineral content.

Materials and Methods

The samples represent a variety of compositions, ranging from basalt host rock, non-ore mineralization to massive sulfide mineralizations. Table 1 provides a detailed description.

No.	Sample name	Material	Bulk porosity	Bulk density (g/cm ³)	Electrical resistivity (Ωm)	Location of origin	Cu	Zn	Fe	Ba	Silica
1	MSM03/2-92DR-5	Basalt	0.080	2.96	124.40	Logatchev	—	—	—	—	—
2	MSM03/2-92DR-2	Basalt	0.016	2.87	70.27	Logatchev	—	—	—	—	—
3	MSM03/2-942DR-1	Gabbro-norite	0.017	3.00	17.79	Logatchev	—	—	—	—	—
4	MSM03/2-942DR-4	Gabbro-norite	0.012	2.93	85.91	Logatchev	—	—	—	—	—
5	MSM03/2-942DR-10	Basalt	0.075	2.94	48.79	Logatchev	—	—	—	—	—
6	SO109/3-49GTV-A-3b	Altered basalt	0.046	2.94	60.40	Axial Smtt	—	—	—	—	—
7	SO157/15DS-1 FG	Basalt	0.275	2.76	31.06	PAR	—	—	—	—	—
8	SO157/17DS-4 FG	Basalt	0.079	2.98	23.87	PAR	—	—	—	—	—
9	SO157/18DS-5-FG	Basalt	0.102	3.07	18.92	PAR	—	—	—	—	—
10	SO157/38DS-Tufat	Basalt	0.074	2.96	19.81	PAR	—	—	—	—	—
11	SO109/2-89GTV-M	Chimney (barite-rich)	0.166	3.65	4.42	Axial Smtt	<1	3	3	34	<0.1
12	SO109/2-89GTV-M (2)	Chimney (barite-rich)	0.176	3.63	6.96	Axial Smtt	<1	3	3	34	<0.1
13	EPR-South	Massive (silica-rich)	0.241	3.29	10.82	SEPR	<1	20	19	<0.1	<0.1
14	SO166/59GTV-A-1B1	Chimney (Zn-Ba)	0.424	4.14	1.99	Pacmanus	<1	50	<1	9	<0.1
15	SO166/70GTV-A-1C4	Massive (Zn-Ba)	0.334	3.79	1.70	Pacmanus	<1	50	2	9	<0.1
16	SO166/70GTV-A-1G1	Massive (Zn-Ba)	0.233	3.93	4.68	Pacmanus	<1	55	3	4	<0.1
17	SO166/58GTV-A-8A1	Massive (Zn)	0.315	4.16	16.13	Pacmanus	<1	53	2	5	<0.1
18	SO208-DR100-2A	Chimney (Zn)	0.302	3.16	3.31	Galapagos	<1	23	12	<0.1	<0.1
19	SO109/2-81GTV-A-211	Chimney (Cu-Zn)	0.360	3.87	0.49	Axial Smtt	12	10	12	<0.1	<0.1
20	SO109/2-81GTV-A-321	Chimney (Cu-Zn)	0.367	4.02	0.28	Axial Smtt	12	10	29	<0.1	<0.1
21	SO166/58GTV-A-2A1	Chimney (Cu-Zn)	0.294	4.13	1.80	Pacmanus	8	23	6	<0.1	<0.1
22	SO166/58GTV-A-6A	Massive (Cu-Zn)	0.405	3.78	0.07	Pacmanus	15	14	11	<0.1	<0.1
23	SO208-DR100-3A	Chimney (Cu)	0.434	3.90	0.11	Galapagos	12	5	29	<0.1	<0.1
24	ODM ROC-V557-324	Chimney (Cu)	0.115	3.94	0.06	Irinovskoe	26	1	25	<0.1	<0.1
25	ODM ROC-V557-327	Chimney (Cu)	0.325	3.40	0.00	Irinovskoe	26	1	25	<0.1	<0.1
26	M64/1-148OV-4E11	Chimney (Cu)	0.424	4.06	0.02	Turtle Pits	22	1	38	<0.1	<0.1
27	M64/1-148OV-4E23	Chimney (Cu)	0.409	3.98	0.09	Turtle Pits	22	1	38	<0.1	<0.1
28	SO109/2-81GTV-A-411	Chimney (Cu)	0.409	4.08	0.36	Axial Smtt	13	2	35	<0.1	<0.1
29	SO109/2-81GTV-A-421	Chimney (Cu)	0.365	4.19	0.17	Axial Smtt	13	2	35	<0.1	<0.1
30	M64/1-124GTV-2E	Chimney (Fe)	0.402	4.23	0.19	Turtle Pits	6	3	37	<0.1	<0.1
31	M64/1-124GTV-2I	Chimney (Fe)	0.381	4.61	0.11	Turtle Pits	6	3	37	<0.1	<0.1
32	M78/2-297ROV-1C	Chimney (Fe)	0.229	3.81	0.84	Turtle Pits	4	1	41	<0.1	<0.1
33	SO157/33GTV-Tufat	Chimney (Fe)	0.279	3.31	0.79	PAR	2	2	34	<0.1	<0.1
34	EPR-sulfide	Chimney (Fe)	0.076	2.80	0.79	SEPR	3	13	31	<0.1	<0.1
35	SO166/58GTV-A-5G	Mineralized breccia	0.266	3.92	3.07	Pacmanus	8	6	5	8	2
36	SO166/70GTV-A-2C1	Mineralized breccia	0.177	2.60	8.33	Pacmanus	<1	3	12	11	1
37	M64/1-139GTV-4A7(1)	Sulfate-rich breccia	0.215	2.62	2.69	Turtle Pits	2	<1	12	<0.1	14
38	M64/1-139GTV-4A7(2)	Sulfate-rich breccia	0.194	2.46	4.05	Turtle Pits	2	<1	12	<0.1	14
39	M64/1-139GTV-7A2(1)	Sulfate-rich breccia	0.128	2.96	2.09	Turtle Pits	6	<1	18	<0.1	10
40	M64/1-139GTV-7A2s	Sulfate-rich breccia	0.246	3.04	2.37	Turtle Pits	6	<1	18	<0.1	10

*Fe present but as silicate phase, not as conductive sulfide; Cu present but as silicate, not as sulfide

Table 1: List of samples with some physical properties and composition (Spagnoli et al., 2016)

The 40 plugs with 25 mm diameter and 50 mm length were measured with the sample holder shown in figure 1. A highly conductive sodium chloride solution with 5 S/m conductivity was used to saturate the samples to simulate the seafloor conditions. In order avoid a current bypass through at the interface between sample and acrylic glass cylinder, the samples were wrapped with teflon tape (figure 1).

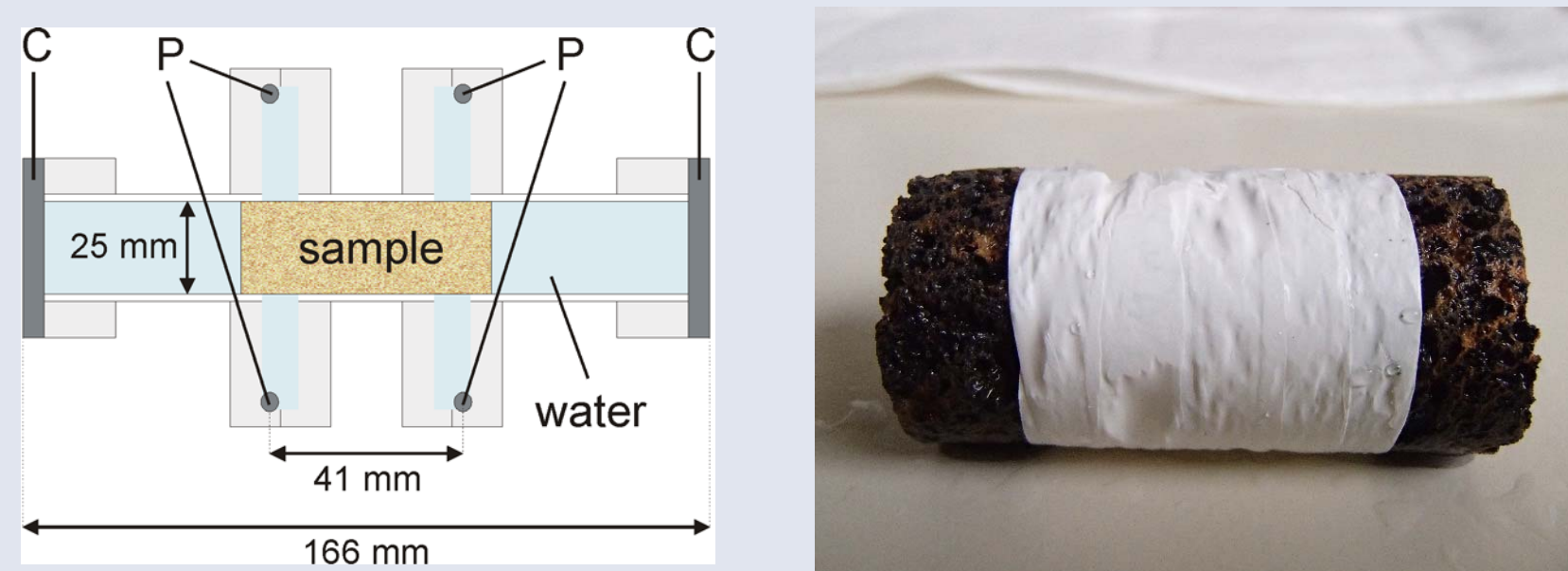


Figure 1. Left: Sketch of the sample holder. Right: SMS sample wrapped with Teflon tape.

Results: Resistivity magnitude

Figure 2A shows the resistivity magnitude at 1 Hz, sorted by sample number, which corresponds to a grouping according to the dominant mineralization type. In particular, the Fe-rich and Cu-rich samples have very low resistivities below 1Ωm, and some even below the resistivity of the fluid used for saturation (0,2 Ωm). The low resistivities cannot be explained by Archie's law (Figure 2B). We conclude that the conducting minerals are connected in these samples.

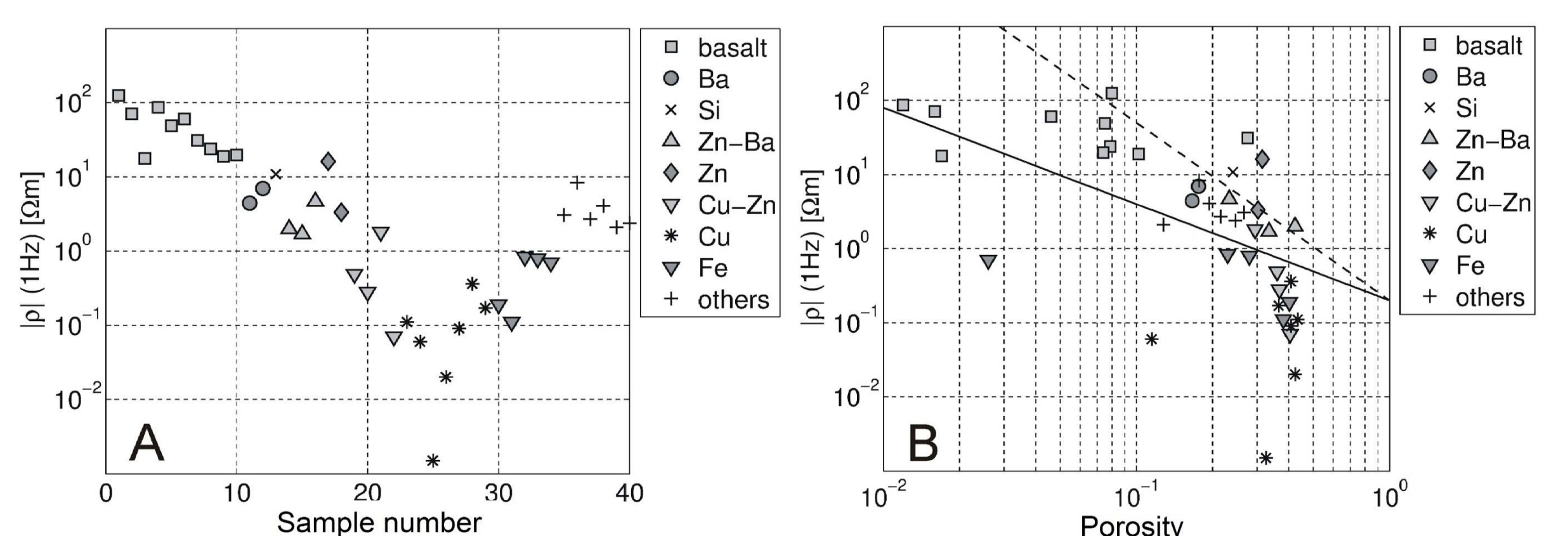


Figure 2: Resistivity magnitude at 1 Hz vs. sample number (A) and vs. porosity (B) (after Spagnoli et al., 2016)). The lines in panel B indicate Archie's law with a=1, m=1,3 (A) and m=2,4 (B).

Results: Imaginary conductivity

The non-mineralized samples have small imaginary conductivities, the sulfides have much larger values, with maxima for the Fe-rich and Cu-rich samples (Figure 3). Compared to the resistivity magnitudes, the discrimination is considerably enhanced. The relationship with porosity (figure 3B) is much weaker.

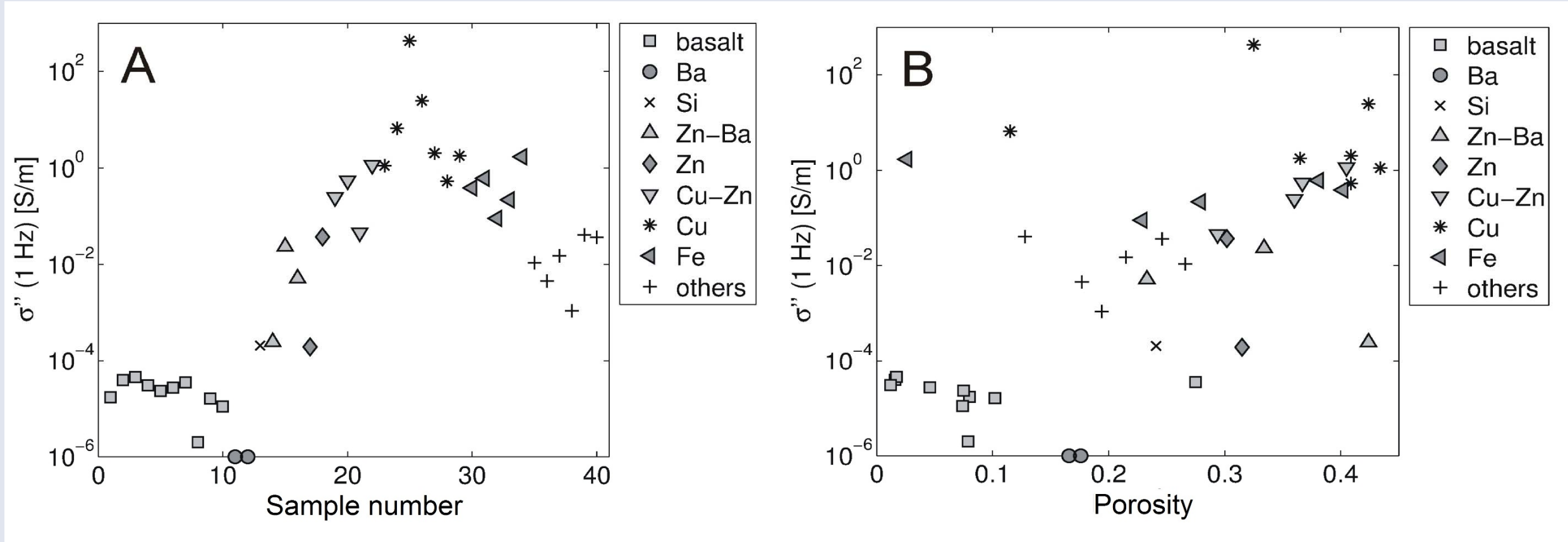


Figure 3: Imaginary conductivity at 1 Hz vs. sample number (A) and vs. porosity (B) (after Spagnoli et al., 2016)).

Saturated and dry spectra

Figure 4 shows 6 selected spectra, 3 of which are for unmineralized, and 3 for mineralized samples. The sulphide-bearing samples generally have large phase shifts in the range of several 100 mrad, and low resistivities, whereas sulfide-free samples have small phase shift and high resistivities.

The samples were also measured under dry conditions. The resistivity magnitudes (figure 5, left panel) have considerably increased. However, the resistivities of two mineralized samples are still small (below 10 Ωm), confirming that the conducting minerals are connected.

The phase shifts of the dry samples (figure 5, right panel) are large. This is unexpected, because it is generally assumed that the electrolyte is essential to generate an IP effect. One hypothesis is that the phase shifts are an artefact caused by coupling or impedance effects. An alternative hypothesis might be that the phase shift is caused by the conducting minerals themselves, without an electrolyte.

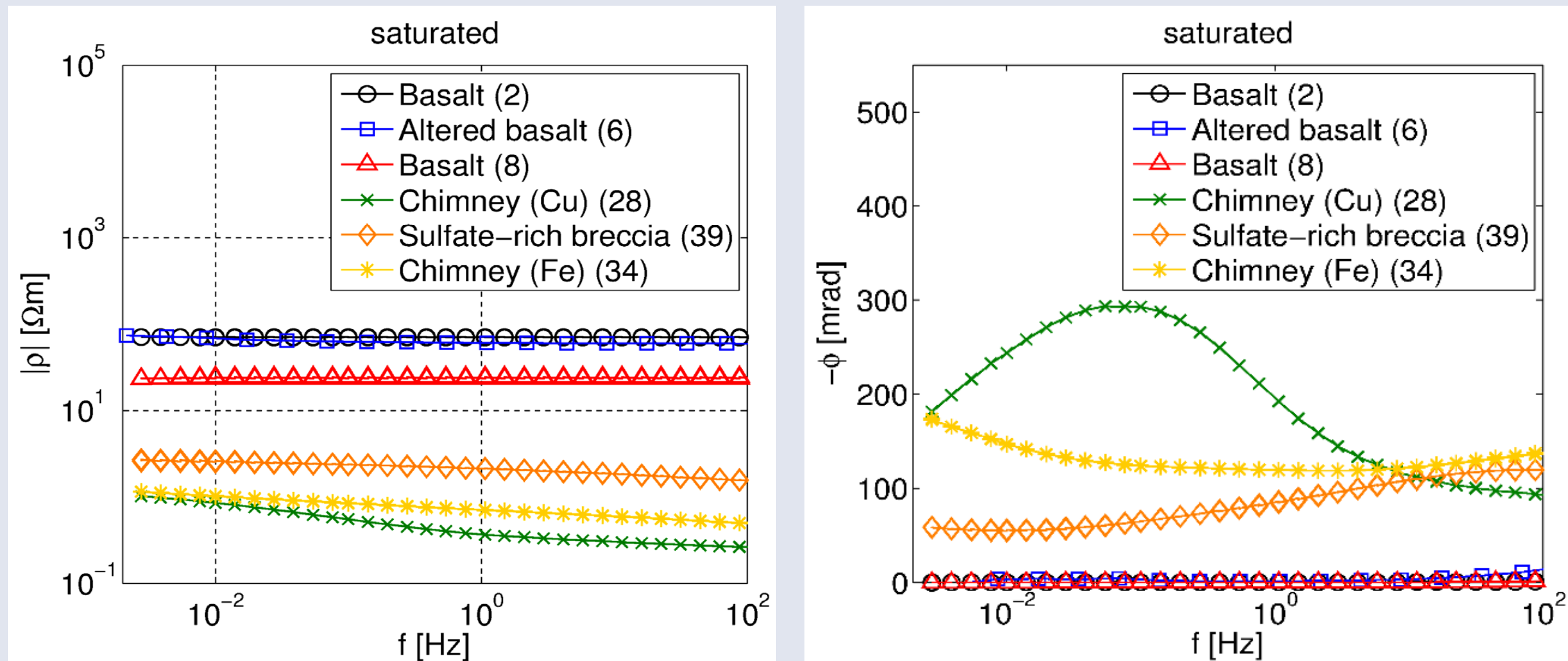


Figure 4. Selected spectra of three samples with no significant sulfide content (basalt samples) and three samples with significant sulfide content, saturated with 5 S/m sodium chloride solution. Top panel: resistivity magnitudes. Bottom panel: phase shift.

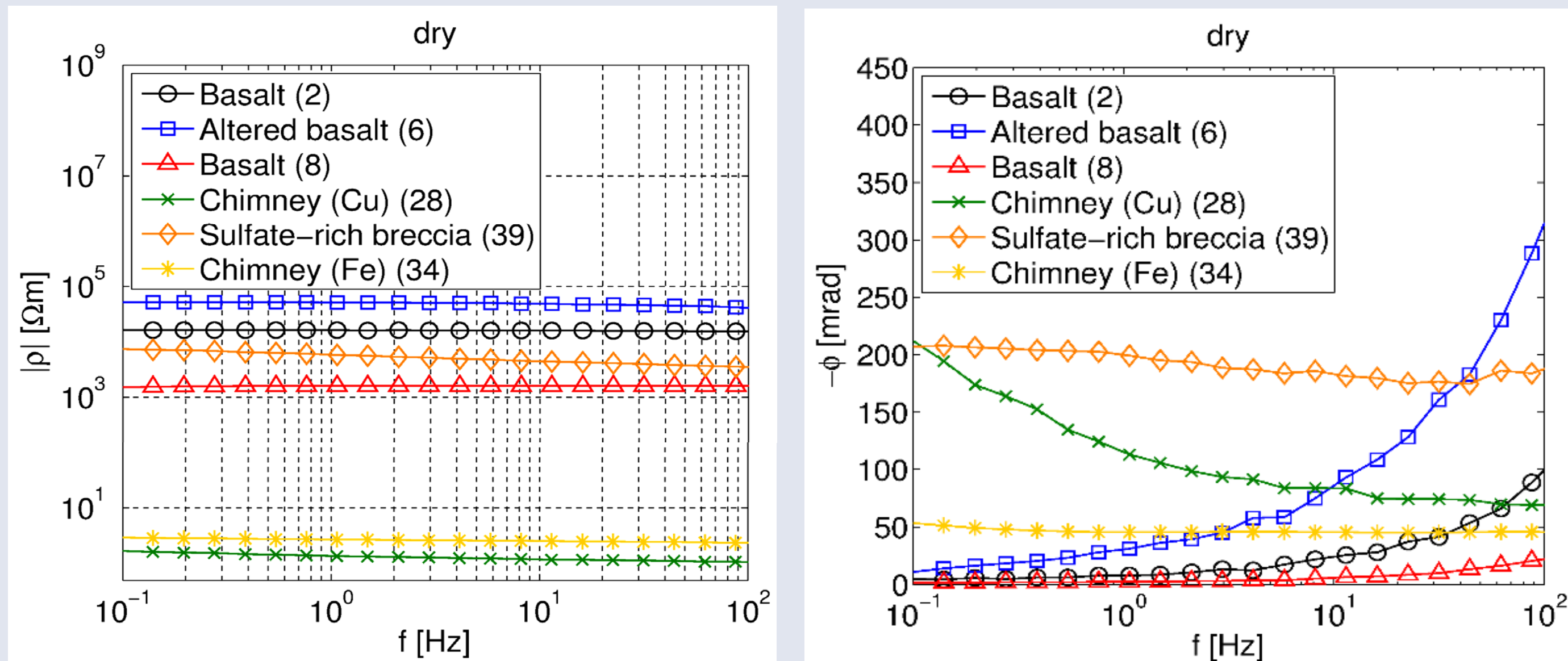


Figure 5. Spectra of the same samples as in figure 4, after drying in a vacuum chamber at 10 mbar and 40°C for at least 24 hours.

CONCLUSIONS

Seafloor massive sulfides show a strong IP effect, i.e. large imaginary conductivities and phase shifts, even under highly saline conditions.

The results indicate that using the imaginary conductivity, even different types of mineralization (e.g. Cu-rich and Fe-rich) might be discriminated. Many of the samples investigated here have resistivities so small that they can not be explained by electrolytic conductivity. We conclude that the minerals in those samples must be connected, and thus the spectra cannot be understood with existing theories, which are based on disseminated minerals (eg. Wong, 1979; Revil et al., 2015).

We also observe large phase shifts for the dry samples. If confirmed, the consequences could be important because existing theories assume the electrolyte as essential to explain IP effects.

ACKNOWLEDGMENTS

The authors thank the Future Oceans research and technology transfer program MaTeP of The Future Ocean Cluster (GEOMAR and CAU Kiel) and BAUER Maschinen GmbH for the financial support for this project and for the permission to publish the results

REFERENCES

Bartetzko A., Klitzsch, N., Itturino, G., Kaufhold, S., and Arnold, J., 2006, Electrical properties of hydrothermally altered dacite from the PACMANUS hydrothermal field (ODP Leg 193): Journal of Volcanology and Geothermal Research 152, 109-120.
Hannington, M., Jamieson, J., Monecke, T., Petersen S., Beaulieu, S. 2011. The abundance of seafloor massive sulfide deposits: Geology 39. 1155–1158.
Pelton, W.H., S.H. Ward, G. Hallof, W.R. Sill, and P.H. Nelson, 1978, Mineral discrimination and removal of inductive coupling with multifrequency IP: Geophysics 43, 588-609.
Revil, A., Florsch, N., Mao, D. 2015, Induced polarization response of porous media with metallic particles -Part 1: A theory for disseminated semiconductors: Geophysics, 80 (5), D525-D538.
Spagnoli, G., Hannington, M., Bairlein, K., Hördt, A., Jegen, M., Petersen, S., and Laurila, T., 2016, Electrical properties of seafloor massive sulfides: Geo-marine letters, DOI 10.1007/s00367-016-0439-5.
Wong, J., 1979, An electrochemical model of the induced polarization phenomenon in disseminated sulfide ores: Geophysics, 44, 1245-1265.